Biophysical Chemistry, 46 (1993) 249–259
Elsevier Science Publishers B.V., Amsterdam

BIOCHE 01743

Model of chemically excitable membranes generating autonomous chaotic oscillations

Nobuko Fuchikami [a,*], Nobuyuki Sawashima [a,1], Masayoshi Naito [b] and Takeshi Kambara [c]

[a] *Department of Physics, Faculty of Science, Tokyo Metropolitan University, Minami-Ohsawa, Hachioji, Tokyo 192-03 (Japan)*
[b] *Advanced Research Laboratory, Hitachi, Ltd., Hatoyama,, Saitama 350-03 (Japan)*
[c] *Department of Applied Physics and Chemistry, The University of Electro-Communications, Chofu, Tokyo 182 (Japan)*

(Received 16 July 1992; accepted in revised form 10 November 1992)

Abstract

A simple mathematical model of the chemically excitable membranes leading to autonomous chaotic oscillations is presented. The model assumes two kinds of autocatalytic ion channels, one is for cations and the other is for anions. Self-consistency between the ion distributions and the electric potentials is taken into account by including the counter ions explicitly. Cations and anions pass through their own channels with their permeabilities changing nonlinearly with the densities of ions at the surfaces of the membrane. Cation and anion transport systems then form two subsystems that oscillate and interact with each other through the membrane potential. When the coupling strength between the two ion systems and adsorption rate of ions to channels are varied, various types of chaotic oscillations are generated autonomously, i.e., without a stimulating periodic force. Experimental evidence to the present model is discussed. It is suggested that endogenous chaos in biological systems may appear from the electric coupling among different kinds of ion transport systems.

Keywords: Chemically excitable membrane; Simulation of membrane oscillation; Autocatalytic channel; Autonomous chaotic oscillation

1. Introduction

There has been increasing attention paid to chaotic oscillations observed in biological systems. These oscillations have been related to pathological phenomena in some cases, such as heart disease [1], epilepsy [2], etc. On the other hand, functional importance of chaos has also been pointed out in connection with biological flexibility. For example, experiments on the olfactory bulb of rabbits show that pre-existing chaotic activity changes to a limit cycle due to recognition of a specific odor [3]. It is also reported that the heartbeat may behave erratically in young and healthy people while increasingly regular behavior sometimes accompanies aging and disease [4]. These experiments together with computer simulations [3] suggest that chaos may be *useful* in enhancing biological variability.

* To whom correspondence should be addressed.
[1] Present address: Research and Development Center, Toshiba Corporation, Komukai Toshiba-cho, Saiwa-ku, Kawasaki 210 (Japan).

Chaotic oscillations are found at various levels of biological complexity: in a single cell unit such as the giant axon of squids [5–10], in a more complex element such as in an aggregate of chicken embryo heart cells [11] and in highly complex systems such as the human brain [12]. In almost all cases the oscillations are related to the membrane potential. In the present paper we propose a possible mechanism of biological chaos by considering chemically excitable membranes as the simplest element of biosystems.

By far chaotic oscillations have been studied more extensively in the electrically excitable membranes than in the chemically excitable ones. Besides in the squid giant axon, chaos was found in internodal cells of *Nitella* [13], *Onchidium* giant neuron [14], *Onchidium* pacemaker neuron [15], and in cardiac pacemakers [11] and in non-pacemaker tissue [16]. In these systems, the membrane potential oscillates chaotically when the systems are driven by a periodic stimulating current. Most of the theoretical work regarding chaotic behavior of membranes has been done based on well-established models of neurons or bursting cells. The most widely studied models are the Hodgkin–Huxley (HH) type oscillators or its modified or simplified versions [17,18]. Using the HH equation, Matsumoto et al. [5] and Aihara et al. [6,7,19] analyzed the action potential of squid giant axon. They reproduced various types of chaotic oscillations which are experimentally obtained when applying a periodic stimulating current. Autonomous (non-driven) chaos has also been found in several theoretical models concerning neuronal or pacemaker activity [20,21,18].

The oscillation phenomena mentioned above arise from the electric excitation of biomembranes induced by various types of voltage-gated ion channels. There exists another type of membrane excitation, that is, the chemical excitation. Chemical stimuli such as neurotransmitters and taste substances induce the oscillation of membrane potential. In some types of chemical oscillation, the oscillations of flow and chemical potential difference of a transported species across a membrane may occur with or without the electric potential oscillation [22,23]. These oscillations may be induced by an allosteric transport protein whose permeability changes nonlinearly with the strength of chemical stimulation [23–25]. Experimentally, self-sustained periodic oscillations of chemically excitable membranes have been studied quite widely using artificial membranes with or even without channel protein. Chaos of this type of membranes has been reported recently as well [26–30]. Theoretically, however, there is not much work done regarding chaotic oscillations of chemically excitable membranes. In contrast to the case of electrically excitable membranes, we do not have well-established models of oscillation like the HH equations. Oscillation phenomena have been explained on a case-by-case basis depending on the individual type of the membrane systems.

The purpose of the present paper is to present a simple mathematical model of chemically excitable membranes and suggest the possibility of self-sustained chaotic oscillations in this type of membranes. The model is a kind of modification of Kawakubo's model [31] in which one kind of ions, cations, are considered that are transported through autocatalytic channels. Here we assume two kinds of autocatalytic ion channels, one is for cations and the other is for anions. By including the counter ions explicitly, the ion distribution and the electric potential are treated selfconsistently. This kind of self-consistency has been taken into account in the refined analysis of steady states [32] but usually ignored in the study of the membrane dynamics.

Computer simulations show that the model generates various types of chaos autonomously, i.e., without stimulating periodic force. It is seen that the present chaos basically originates from the coupling between different kinds of self-oscillating ion systems. The results obtained suggest that endogenous chaos in membrane systems may appear from the electrical coupling among the periodically oscillating subsystems.

2. Model

We consider a model system in which a membrane is in aqueous solution containing ions and

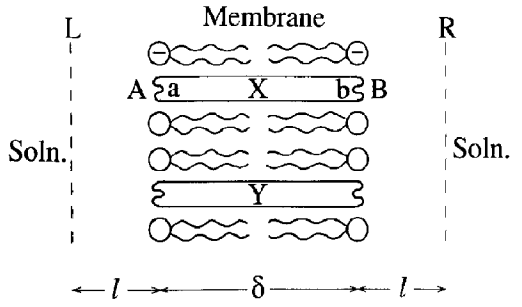

Fig. 1. Model of chemically excitable membrane. The membrane has negative charges $-e\sigma_m$ on its surfaces. X: cation channel. Y: anion channel. The channels are autocatalytic. Distribution of the channels is averaged over the membrane. a, b: ion adsorption sites to the channels. A, B: surfaces of the membrane. L, R: planes introduced to screen net surface charges. Regions outside L and R are electrically neutral bulk solution regions. Ions are assumed to be located on four sites A, a, b, B except for bulk solutions.

divides the solution into two regions. The ion species considered are a kind of monovalent cation X^+ and a kind of monovalent anion Y^-.

We further assume that the membrane consists of lipid molecules and channel protein. But we note here that should we read 'pore channel' for 'channel protein', the present model can be extended to synthetic lipid membranes, such as millipore filters impregnated with dioleyl phosphate (DOPH), which do not have a specific channel protein. Lipid molecules form a bilayer having negative charges on the surfaces of the membrane and channel protein provides transport pathways for ions through the membrane.

The model system is shown in Fig. 1. (This figure corresponds to the biomembrane, not to the millipore membrane.) There are autocatalytic channels for cations and anions. We consider a uniform membrane with the distribution of channels averaged over the membrane. A and B are the outer surfaces of the membrane, respectively, whilst a and b are the adsorption sites of ions to channels. The membrane of thickness δ has negative surface charges. The density of these charges is $-e\sigma_m$. Because of these surface charges, densities of ions at the surfaces A and B are different from those in the bulk solutions. We write the areal densities of cations at the surfaces X_A, X_B, and those of anions Y_A, Y_B. Since the electric conductivity of the electrolyte is much larger than that of the membrane, it is reasonable to assume that the excess charges of the membrane are screened completely at any time so that there is no net charge everywhere far enough from the membrane. We approximate the screening by introducing planes L and R as in the Helmholtz model, that is, screening charges near the surfaces are assumed to be located discretely on L and R. For simplicity, we assume that the widths of the layers LA and RB are the same, i.e., $l = \overline{LA} = \overline{RB}$, where l is of the order of screening length. Regions outside of the planes L and R are the bulk solution regions. The transport of ions through the channels is described by a single barrier model [32] in which ions jump over a single activation energy barrier between a and b. Thus, ions are assumed to be only on the four sites (thin sheets of thickness λ) located at A, a, b, and B, except for two bulk solution regions. Ions move between two bulk solution regions through these sites under the influences of concentration differences of ions and the membrane potential. The movement of ions in turn affects the membrane potential. Ion concentrations in the bulk solutions are held constant, and the bulk solutions serve as the source and drain of ions to drive the system.

We describe the dynamics of the system in terms of the kinetic constants specifying the following processes.

$$\mathrm{L} \underset{d_{\mu 1}^-}{\overset{d_{\mu 1}^+}{\rightleftharpoons}} \mathrm{A} \underset{k_{\mu a}^-}{\overset{k_{\mu a}^+}{\rightleftharpoons}} \mathrm{a} \underset{d_{\mu 2}^-}{\overset{d_{\mu 2}^+}{\rightleftharpoons}} \mathrm{b} \underset{k_{\mu b}^+}{\overset{k_{\mu b}^-}{\rightleftharpoons}} \mathrm{B} \underset{d_{\mu 3}^-}{\overset{d_{\mu 3}^+}{\rightleftharpoons}} \mathrm{R} \qquad (1)$$

where μ denotes ion species and $\mu = \mathrm{X}$ for cation and $\mu = \mathrm{Y}$ for anion. The temporal changes of the ion distributions in the kinetic processes (1) are determined by the following rate equations.

$$\frac{dx_j}{dt} = I_{X,j} - I_{X,j+1}, \ (j = 1 \sim 4),$$

$$\frac{dx_{j+4}}{dt} = I_{Y,j} - I_{Y,j+1}, \ (j = 1 \sim 4), \qquad (2)$$

where $(x_1, \cdots, x_8) = (X_A, X_a, X_b, X_B, Y_A, Y_a, Y_b, Y_B)$ and $I_{\mu,j}$s are ion fluxes expressed by

$$I_{X,1} = d^+_{X1} X_l - d^-_{X1} X_A,\ I_{X,2} = k^+_{Xa} X_A - k^-_{Xa} X_a,$$
$$I_{X,3} = d^+_{X2} X_a - d^-_{X2} X_b, \text{ etc.} \quad (3)$$

Here, X_ν (ν = A, a, b, B) is the areal density of cations at the site ν, Y_ν is that of anions, and X_l and X_r denote that X_l/λ and X_r/λ are the cation concentrations in the left and right bulk solutions, respectively, which are held constant. Because of the electro neutrality in the bulk solutions, anion concentrations are equal to cation concentrations there, that is, $Y_l = X_l$ and $Y_r = X_r$.

The kinetic constants $k^+_{\mu\gamma}$s (γ = a, b) represent the adsorption rate of ions to the channels and $k^-_{\mu\gamma}$s represent the desorption rate. A basic assumption in the present treatment is that these parameters are not constant but increasing functions of ion densities because the channels are autocatalytic. We employ the simplest form:

$$k^\pm_{X\gamma} = k^\pm_{X0} + k^\pm_{X2}(X_\gamma)^2,$$
$$k^\pm_{Y\gamma} = k^\pm_{Y0} + k^\pm_{Y2}(Y_\gamma)^2, \quad (4)$$

where the second terms correspond to a third-order autocatalytic process as

$$X_A + 2X_a \underset{k^-_{X2}}{\overset{k^+_{X2}}{\longrightarrow}} 3X_a. \quad (5)$$

which was assumed also in Kawakubo's model [31]. As pointed out by Nicolis and Prigogine, at least a third-order nonlinear process is necessary for the system to oscillate [33]. Justification of eq. (4) will be discussed later on.

Since there exist electric fields between the sites L and A, a and b, and B and R due to the charges located on the sites, the effect of these fields on movement of ions can be taken into account by modifying $d^\pm_{\mu i}$ (i = 1, 2, 3) as

$$d^\pm_{\mu i} = d_{\mu i} \exp(\pm z_\mu e\beta\phi_i/2), \quad (6)$$

which we approximate by

$$d^\pm_{\mu i} = d_{\mu i}(1 \pm z_\mu e\beta\phi_i/2), \quad (7)$$

where ϕ_i is the potential difference at region i, $\beta = 1/k_B T$ is the inverse of temperature, and z_μ is the valence of ion μ. $d_{\mu i}$ is effectively the diffusion constant of ions in each region. ϕ_1 and ϕ_3 are the surface potentials and ϕ_2 corresponds to the diffusion potential. Equation (6) is exact only in the equilibrium states but often is assumed exact in the non-equilibrium state as well [32,31]. From the Poisson equation, the potentials are expressed in terms of charge densities as

$$\phi_1 = \phi_L - \phi_A = el\sigma_L/\epsilon_w,$$
$$\phi_2 = \phi_a - \phi_b$$
$$= e\delta(\sigma_L + X_A - Y_A + X_a - Y_a - \sigma_m)/\epsilon_m, \quad (8)$$
$$\phi_3 = \phi_B - \phi_R = -el\sigma_R/\epsilon_w,$$

where ϵ_w and ϵ_m are the dielectric constants of water and the membrane, respectively, $e\sigma_L$ and $e\sigma_R$ are the charges which appear on the planes L and R to screen the net surface charges of the membrane.

There are nine independent variables in the present system. There are cations and anions on the planes A, a, b, and B, that is, X_νs and Y_νs, and charges on the planes L and R. These ten variables are not mutually independent, since the following relationship holds because the total charge of the system is zero (charge neutrality for the whole system).

$$\sigma_L + \sigma_R + \sum_\nu (X_\nu - Y_\nu) - 2\sigma_m = 0 \quad (9)$$

The number of equations derived from the kinetics is eight as seen in eq. (2). An additional equation that is necessary to complete the description of the system is obtained from the current continuity condition, i.e. the electric current through the membrane system is equal to the current applied to the system by an external circuit. The electric current in the membrane is the sum of ionic current $e(I_{X,3} - I_{Y,3})$ and displacement current $d(\epsilon_m\phi_2/\delta)/dt$. Then we obtain a relation

$$\frac{d}{dt}\left(\frac{\epsilon_m}{e\delta}\phi_2\right) = -I_{X,3} + I_{Y,3} + I_0, \quad (10)$$

where eI_0 is the electric current density applied to the system. Current continuity is guaranteed

throughout the system by the mass balance equations (2).

We take X_ν, Y_ν (ν = A, a, b, B) and ϕ_2 as independent variables, and solve time evolution equations (2) and (10) numerically. Then the surface potentials ϕ_1 and ϕ_3 in $d_{\mu 1}^{\pm}$ and $d_{\mu 3}^{\pm}$ are expressed in terms of the independent variables using eqs. (8) and (9). In this way, we obtain at every second the ion densities and the potentials.

In the present model, motions of cations and anions couple through membrane potential with the inverse temperature coupling constant, β. If β is non-zero, diffusion rate $d_{\mu i}^{\pm}$ for ion μ (μ = X or Y) contains ϕ_i as in eq. (7). Because the ϕ_is (i = 1, 2, 3) are the potential differences due to charges on the sites where ions are present, they are functions of both cation densities X_νs and anion densities Y_νs as seen from eqs. (8) and (9). Thus the motion of cations affects the motion of anions and vice versa through the ϕ_is. The membrane potential ϕ_m comprises ϕ_is as

$$\phi_m = \phi_1 + \phi_2 + \phi_3. \tag{11}$$

In the limit of $\beta = 0$, $d_{\mu i}^{\pm}$s reduce to constants $d_{\mu i}$s. Then the equations for $x_1 \sim x_4$ ($x_5 \sim x_8$) in eq. (2) contain only cation (anion) densities, and the cation and anion systems are decoupled. Cations and anions move independently with each other. Physically the condition $\beta = 0$ corresponds to the situation where thermal motion of ions predominates over the effect of electric field at infinite temperatures. In the following, we use a normalized parameter $\beta' = T_0/T$ with $T_0 = 298$ K for the inverse temperature.

Although the basic equations (2) and (10) describing the system behavior include various kinds of parameters, there are several scaling properties among them. In this sense, the choice of the values of the parameters is rather arbitrary. For example, if a solution $x(t) = (X_A(t), \ldots, X_B(t), Y_A(t), \cdots, Y_B(t), \phi_2(t))$ is obtained for a set of parameters (X_l, X_r, σ_m, β, $d_{\mu i}$, $k_{\mu\gamma}^{\pm}$), solution $x(t)/\alpha$ with an arbitrary constant α is obtained corresponding to the changes of the parameters $X_l \to X_l/\alpha$, $X_r \to X_r/\alpha$, $\sigma_m \to \sigma_m/\alpha$, $\beta \to \alpha\beta$, $k_{X2}^{\pm} \to \alpha^2 k_{X2}^{\pm}$, and $k_{Y2}^{\pm} \to \alpha^2 k_{Y2}^{\pm}$, the rest of the kinetic constants remaining unchanged.

3. Computational results

3.1. Autocatalysis assumed only for cation channels

Before going on to the case where both the cation and anion channels are autocatalytic, we mention here briefly the results of the calculation for the case where autocatalysis is assumed only for cation channels. We set here the surface charge σ_m to be zero. Thus the results are symmetric when autocatalysis is assumed only for anion channels.

3.1.1. No coupling limit

As mentioned previously, cation and anion systems decouple in the limit $\beta' \to 0$. In this limit, the cation system coincides with Kawakubo's periodically oscillating system [31] in the same limit. For certain values of the parameter set, cation densities X_νs oscillate periodically, while anion densities Y_νs take on stationary values. Adequate values of parameters are required to render the system oscillatory. We can obtain these values by imposing the condition that the cubic equation $I_{X,2} = 0$ (or $I_{X,4} = 0$) for X_a (or X_b) has three real roots. The values are not unique.

3.1.2. Effect of the coupling

Coupling between cation and anion was introduced by putting β' to 1. It was found that coupling has two opposite effects depending on which of cation transport or anion transport is rate limiting. When the rate constants of anions are much larger than those of cations and the motion of the latter is rate limiting, the oscillation of cation densities are enhanced by the coupling, that is, amplitude becomes larger and frequency becomes higher. On the other hand, in the opposite case where the motion of anions is rate limiting, the coupling keeps the cation system from oscillating.

3.1.3. Effect of an external d.c. current

When an external d.c. current is applied to the oscillating system from the more concentrated solution side to the dilute side, the oscillation is generally enhanced. In some cases the current

can also induce oscillations in an otherwise non-oscillating system.

3.2. *Autocatalysis assumed both for cation and anion systems*

When both cation and anion channels are autocatalytic, the present system shows various types of chaotic oscillations in ionic concentrations and potentials as well as sustained periodic ones under an ionic concentration gradient. Values of parameters employed in the calculation are summarized in Table 1. The ion concentrations in the bulk solutions were adjusted to the values listed in Table 1, that is, the concentration X_l/λ in the left side solution was 17.5 mM and that in the right side solution, X_r/λ, was 0.5 mM. We hereafter use the units for constants and variables shown in the table. The external current I_0 was set zero, i.e., there was no external oscillating forces. This condition makes the present system autonomous one. Examples of oscillating waveforms are shown in Fig. 2. The waveforms of cation density X_A and anion density Y_A at the membrane surface A are plotted for $\beta' = 1$ and four values of k^+_{Y0}. The oscillations are period 1 ($k^+_{Y0} = 0.127$), period 2 ($k^+_{Y0} = 0.128$), period 4 ($k^+_{Y0} = 0.129$), and chaos ($k^+_{Y0} = 0.12924$).

We took β' and k^+_{Y0} as control parameters. First, the value of β' was varied to investigate the effects of coupling the two kinds of ions. Second, we examined how the behavior of the system changed when the value of k^+_{Y0}, which is the zero order adsorption rate constant of anions to channels, was changed. Other kinetic rate constants were fixed at the values in Table 1. The fixed

Table 1

Data used in the simulation

Quantities	Values
(δ,l,λ) in nm	(5,10,0.1)
(X_l,X_r,σ_m) in nm.mM	(1.75,0.05,0.5)
$(d_{X1},d_{X2},d_{X3},k^+_{X0},k^-_{X0})$ in s^{-1}	(0.2,1.1,2.0,0.13,2.0)
(k^+_{X2},k^-_{X2}) in s^{-1} (nm mM)$^{-2}$	(10.4,6.4)
$(d_{Y1},d_{Y2},d_{Y3},k^+_{Y0},k^-_{Y0})$ in s^{-1}	(0.3,1.5,2.8,−,2.8)
(k^+_{Y2},k^-_{Y2}) in s^{-1} (nm mM)$^{-2}$	(14.8,8.8)
(ϵ_w,ϵ_m) in 10^{-10}F/m	(6.93,2.772)

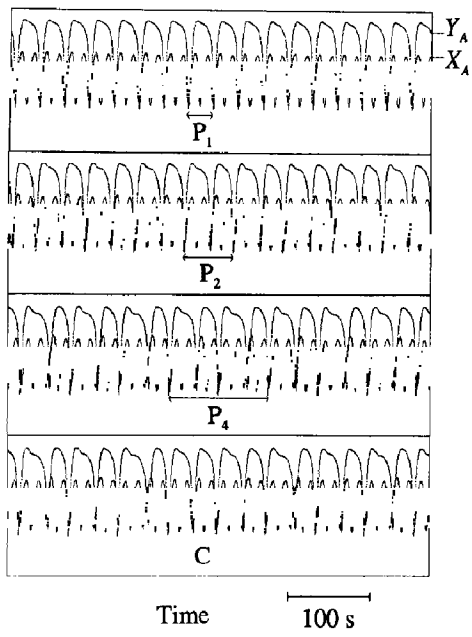

Fig. 2. Oscillating waveforms of cation density X_A and anion density Y_A at the surface A. Ordinate: $0.5 \le X_A, Y_A \le 1.5$. P_1: $k^+_{Y0} = 0.127$, P_2: $k^+_{Y0} = 0.128$, P_4: $k^+_{Y0} = 0.129$, C: $k^+_{Y0} = 0.12924$.

value $\beta' = 1$ was used. By this procedure, we investigated how the change in a parameter of one of the subsystems affects the global behavior of the system.

It is shown that various types of transitions between periodic and chaotic oscillations appear. These include collapse of quasiperiodicity, period doubling bifurcations, intermittency, and alternating periodic–chaotic sequence which are observed in forced electrically excitable membranes such as squid giant axon [5–10,19].

3.2.1 *Chaos from quasiperiodic motions*

Here, we fix k^+_{Y0} at 0.12924 and vary β'. The case of $\beta' = 1$ corresponds to the chaos C in Fig. 2.

When $\beta' = 0$ the system oscillated quasiperiodically. As β' was increased, the transitions from quasiperiodic to chaotic motions through periodic ones were observed. The result shows that coupled motion of two kinds of ions is essetial in creating chaos. When $\beta' = 0$, the present system decouples into two subsystems. One is the system of cations with variables (X_A, X_a, X_b,

X_B), and the other is the system of anions with variables (Y_A, Y_a, Y_b, Y_B). The subsystems oscillate only periodically, independently from each other. These two types of periodic oscillations of subsystems give rise to a quasiperiodic oscillation as a whole. As β' is increased from zero, the oscillations become coupled and the oscillation of the whole system becomes periodic by frequency locking and then chaotic oscillations result.

3.2.2. Bifurcation diagram

Figure 3 is the bifurcation diagram when β' is fixed at 1 and k_{Y0}^+ is varied in the range $0.106 \leq k_{Y0}^+ \leq 0.138$. In the figure, values of the minimum points of oscillating Y_A are plotted. n Lines denote period n oscillation and a band denotes chaotic oscillation. It is seen from the figure that the present system exhibits various types of oscillations and transition sequences between them when a parameter of one of the subsystems is changed. For example, there is a a complicated structure in the range $0.1295 \leq k_{Y0}^+ \leq 0.135$ which we have not yet analyzed completely. The complicated structure of the bifurcation diagram would be due to the large number of freedom (9-variables) in the present system.

The diagram was obtained as follows. We started simulation with the control parameter k_{Y0}^+ of 0.106 and the initial condition (X_A, X_a, X_b, X_B, Y_A, Y_a, Y_b, Y_B, ϕ_2) = (X_l, σ_m, σ_m, X_r, X_l, 0, 0, X_r, 0). After a transient period, a periodic oscillation was obtained for which we plotted the minimum value of Y_A at each period. Then, we increased k_{Y0}^+ by a certain amount and started the second simulation using the final state obtained in the previous simulation as the initial state. The same procedure was repeated afterwards. When k_{Y0}^+ reached 0.138, the procedure was continued backward decreasing the value of k_{Y0}^+.

The diagram shows that there is a hysteresis around $k_{Y0}^+ \approx 0.109$. There, the solid lines correspond to the case where k_{Y0}^+ is increased and the dotted lines correspond to the case where it is decreased. Oscillations of period 1 and period 4 coexist in the range $0.1085 \leq k_{Y0}^+ \leq 0.1099$. For other transitions, no hysteresis was observed. For example, at the transition point $k_{Y0}^+ = 0.1195$, two of three peaks of the period three oscillation continuously merge into one.

3.2.3. Period doubling sequence

A period doubling sequence is observed around $k_{Y0}^+ \approx 0.129$. Figure 4 shows a bifurcation diagram in the range $0.1275 \leq k_{Y0}^+ \leq 0.1295$. As k_{Y0}^+ is increased, period doubling bifurcations occur, accumulating to chaos. P_2, P_4 and C correspond to the three respective cases in Fig. 2. In Fig. 5, the

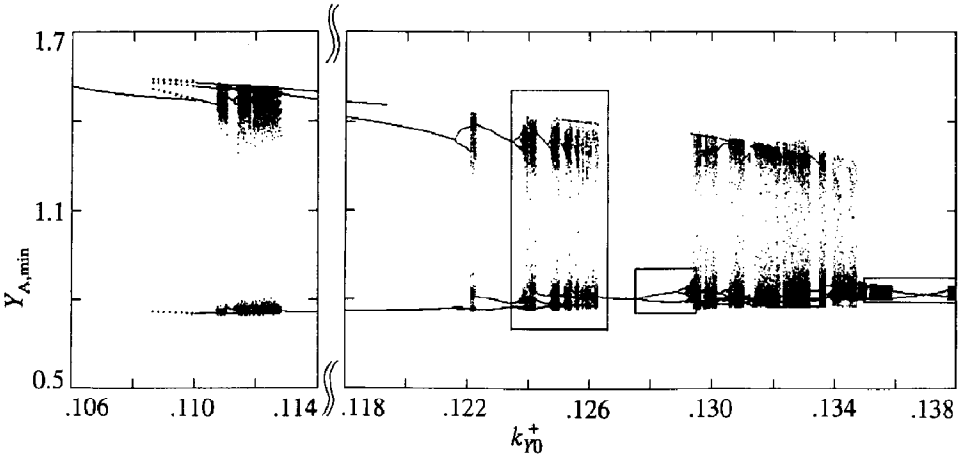

Fig. 3. Bifurcation diagram where the minimum values $Y_{A,min}$s of oscillating Y_A are plotted for each value of k_{Y0}^+. n lines denote period n oscillation and band denotes chaotic oscillation. $\beta' = 1$. At around $k_{Y0}^+ \approx 0.109$, solid (dotted) lines correspond to the case where the calculation is done with increasing (decreasing) the value of k_{Y0}^+. Regions enclosed in cadres are shown enlarged in figs. 4, 7(a), and 8.

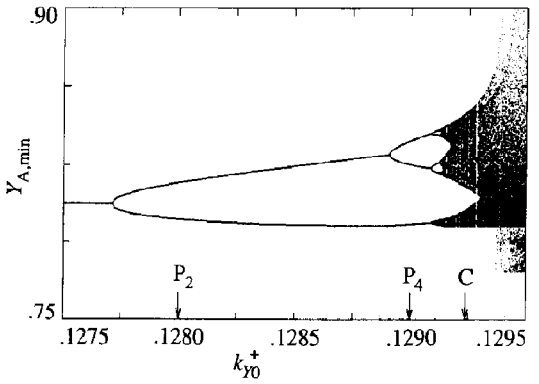

Fig. 4. Bifurcation diagram including period doubling. P_2, P_4 and C correspond to the three respective cases in Fig. 2.

power spectra of $Y_A(t)$ at P_1, P_4, P_{16} (k^+_{Y0} = 0.12913) and C are presented. Subharmonics with period 2 and 4 appear in P_4 and subharmonics with period 2, 4, 8 and 16 in P_{16}. The waveform of C does not seem to be very different from P_4 in Fig. 2, but the difference in spectrum between C and even P_{16} is clear. In Fig. 6, chaotic attractor corresponding to C is shown. Figure 6(a) is the projection of the attractor in the case of k^+_{Y0} = 0.12924 onto the (X_A, Y_A) plane, and Fig. 6(b) is the Poincaré section, i.e., the return map of Y_A. The map was made by plotting ($Y_{A,1}$, $Y_{A,2}$), ($Y_{A,2}$, $Y_{A,3}$), $\cdots$, where $Y_{A,n}$ is the nth minimum point of the oscillation of Y_A. Although the trajectory in Fig. 6(a) is complicated because it is the projection of the full trajectory in a nine-dimensional space onto a two-dimensional plane, the feature of the attractor is readily seen from the Poincaré section (Fig. 6b). It is seen that the Poincaré section looks like a "line" which suggests the fractal dimension of the section to be close to unity. We calculated the correlation dimension

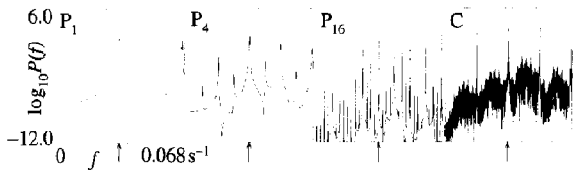

Fig. 5. Power spectral density $P(f)$ of Y_A at P_1, P_4, P_{16}: k^+_{Y0} = 0.12913 and C. P_1, P_4 and C correspond to the three respective cases in Fig. 2. Arrows indicate the fundamental frequencies $f \approx 0.0336\ s^{-1}$.

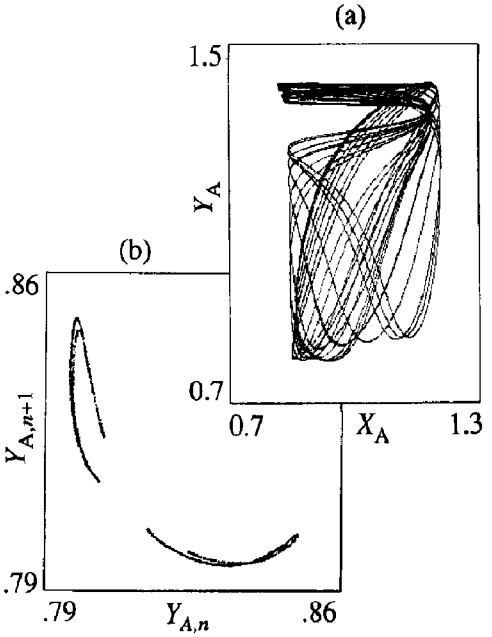

Fig. 6. (a) Chaotic attractor projected onto the (X_A, Y_A) plane. (b) Return map of Y_A. k^+_{Y0} = 0.12924. In the return map, successive values of the minimum points of Y_A are used.

[34] of the section and actually obtained a value nearly unity. The dimension d is 1.07 in case of k^+_{Y0} = 0.12924, d = 1.12 for k^+_{Y0} = 0.12930, and d = 1.24 for k^+_{Y0} = 0.12936. The dimension of the attractor in the full phase space is $D = d + 1$.

3.2.4. *Intermittency*

In Fig. 7(a), we see the transition between periodic oscillation and intermittent chaos at $k^+_{Y0} \approx 0.1359$. Figure 7(b) shows the return map of the membrane potential ϕ_m at k^+_{Y0} = 0.1358. The map essentially consists of two parts, a lower left part with dense points and an upper right part with less dense points, reflecting the intermittency. This reminds us of a similar map as obtained from the heartbeats of a healthy heart, where a $1/f$-like spectrum is observed [4]. It is well known that the intermittent chaos has $1/f$ spectrum [35]. Detailed analysis of the present intermittency is now in progress.

3.2.5. *Period–chaotic transition sequence*

In the bifurcation diagram, Fig. 3, we observe a self-replicating structure where periodic regimes

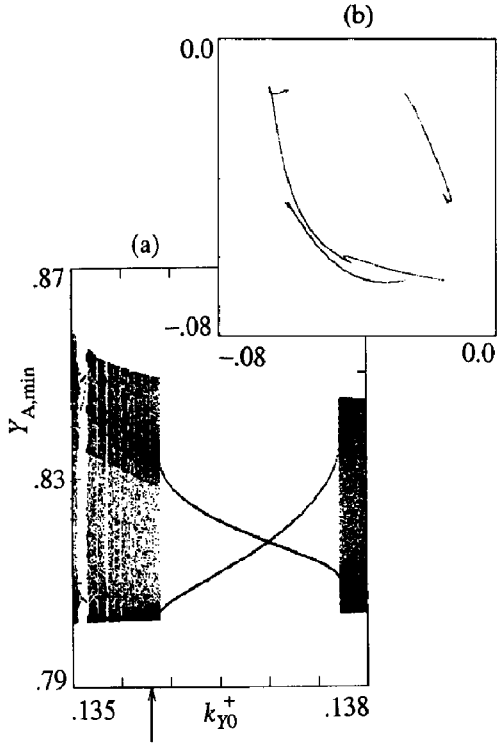

Fig. 7. (a) Bifurcation diagram including intermittent chaos. (b) Return map of the normalized membrane potential $e\beta\phi_m$ at $k_{Y0}^{+} = 0.1358$ (indicated by an arrow in (a)). In (b), successive values of the minimum points of $e\beta\phi_m$ are used.

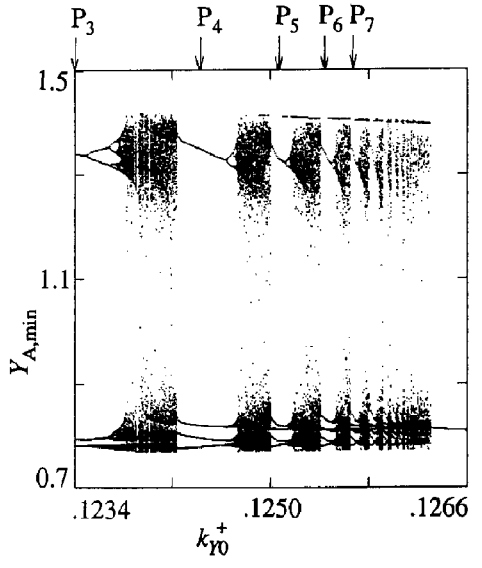

Fig. 8. Alternating periodic–chaotic sequence. Starting from period 3, periodic and chaotic oscillations appear alternatingly as: period $n \rightarrow$ chaos $\rightarrow$ period $n+1 \rightarrow$ chaos when the value of k_{Y0}^{+} is increased.

and chaotic regimes appear alternatingly in the range $0.1234 \leq k_{Y0}^{+} \leq 0.1263$. Figure 8 is the bifurcation diagram covering this range. At $k_{Y0}^{+} = 0.1234$, the oscillation is period 3. When the control parameter k_{Y0}^{+} is increased, the oscillation becomes chaotic, and afterwards, chaotic and periodic oscillations appear such that chaos $\rightarrow$ period $n \rightarrow$ chaos $\rightarrow$ period $n+1$. Each route to chaos is period doubling. The alternating appearance of periodic and chaotic regimes is a kind of alternating periodic–chaotic transition sequence [36].

4. Discussion

We have analyzed a model of chemically excitable membrane. The model is a kind of modified version of Kawakubo's [31]. In fact, he considered the DOPH millipore membrane. In this sense, the present model may be more directly connected with this kind of artificial membrane, if 'pore channel' is read for 'channel protein'. As is seen from Fig. 3, the bifurcation structure of eqs. (2) and (10) are considerably complicated in comparison with three- or four-variable systems. The system is, however, regarded as composed of two kinds of subsystems, a cation and an anion system which couple electrically with each other. In order for the oscillations to be sustained without damping, at least a third-order nonlinear term (proportional to $-x_i^3$) should be included in $f_i(x_1, x_2, \ldots)$ in the time evolution equation $dx_i/dt = f_i(x_1, x_2, \ldots)$ [33]. This nonlinearity is introduced phenomenologically as eq. (4) by assuming autocatalytic processes in the interface region.

Direct experimental evidence justifying eq. (4) itself has not been obtained so far. However, there are several experiments which may be regarded as indirect supports. One is concerned with a nice episode about theoretical and experimental studies pursued by Yoshida and coworkers: Before the discovery of the self-sustained oscillations of DOPH millipore membranes [37], it was experimentally known that the membrane exhibits hysteresis in the permeability

of salt. Then that was traced to a conformation change occurring in the DOPH layers in the pores on the membrane [38]. Based on this observation, it was predicted that oscillations may occur, which was in fact found subsequently Miyake and Kurihara indicated from experiments on the mouse neuroblastoma cell (N-18) that K^+ channels in N-18, which are not the voltage-dependent ones, are open at high concentration of K^+ and close at low concentration [39]. Heinemann and Sigworth measured the fluctuation in the current through gramicin A channels and showed that the presence of bound ions stabilizes the high conductance conformation of the channel [40]. Taking account of these experiments, it is plausible to consider that the nonlinear change of the membrane permeability induced by the conformation change of the channels is reflected in the autocatalytic equation (4). pH oscillations of artificial membrane imbedded with immobilized enzyme as channel protein was also explained theoretically by assuming autocatalytic channels [41].

The nonlinearity above mentioned is a condition for the oscillating motion, but for oscillations to be chaotic this is not enough, even though we have four variables in the single ion system. In general, four degrees of freedom are enough to generate chaos. But this does not work here. Four variables of the present system are obtained from just one kind of ion density $c(x)$ by taking discrete points on the space coordinate x. The ion density at each site couples only with those at the nearest neighbor sites. For the system to generate chaos autonomously, the coupling between ion densities at the non-nearest neighbor sites is necessary, which is quite unphysical. The chaotic motion is induced in the present problem through the coupling of two oscillating systems. We have considered cation X^+ and anion Y^- explicitly. To be more realistic, we could include two kinds of cations X^+ and X'^+, corresponding to Na^+ and K^+ for example, apart from Y^-. To extend the present model in this way is straightforward. Even in this case, the motions of three subsystems of X^+, X'^+, Y^- are separated in the limit $\beta \to 0$. Thus, if nonlinearity is assumed so that at least two kinds of ion systems can oscillate, quasiperiodic–chaotic transitions may occur if β is increased. Again in the experiment on DOPH membrane, it is indicated that the membrane can discriminates Na^+ from K^+ [42]. This suggests that non-driven chaos is not impossible under the circumstance that both ion systems are oscillatory.

Recently chaotic oscillation of DOPH membrane under a sinusoidal stimulating current were observed in the presence of a KCl-concentration difference [28,29]. There are also several experiments on autonomous chaos of millipore membranes. Hayashi et al. [27] observed chaotic oscillations of DOPH membrane induced by a constant current, where the membrane is placed between KCl aqueous solutions. They investigated the effect of taste substances added to the aqueous solutions. The waveform and the correlation dimension of the chaotic attractor are sensitive to the current intensity and the taste substances. Uemura and Ishii used a membrane doped with triolein which is placed between NaCl and KCl solutions [26]. No external current is applied. Periodic self-oscillations become aperiodic when the membrane contains a larger amount of triolein. They made another experiment using a membrane doped with sorbitan monooleate and concluded that aperiodic self-sustained oscillation is intermittent chaos [30].

We proposed a simple model of chemically excitable membranes and showed the possibility of autonomous chaos in this type of membrane. The present theory may also serve as a "metaphor" in Rosen's definition [43] for biological chaos. It is suggested that chaotic behavior in the autonomous biological systems can be generated through the coupling among autonomously periodic subsystems. Periodically oscillating systems are commonly encountered in biological systems. Among them, those systems which generate chaos under stimulating periodic forces would be the probable candidates for the systems which give rise to endogenous chaos when they are coupled. It is probable that the systems couple each other through membrane potential and/or ionic or molecular environment of the solutions.

Acknowledgments

A part of the work was done when one of the authors (N.F.) stayed in Hungary. She would like to thank Professor F.J. Kedves and the members of his group of Kossuth Lajos University for their warm hospitality granted to her at that period.

References

1 L. Glass, A. Shrier and J. Bélair, in: Chaos, ed. A.V. Holden (Manchester Univ. Press, Manchester, 1986) p. 237.
2 A. Babloyantz and A. Destexhe, Proc. Natl. Acad. Sci. USA 83 (1986) 3513.
3 C.A. Skarda and W.J. Freeman, Behav. Brain Sci. 10 (1987) 161.
4 A.L. Goldberger and D.R. Rigney, in: The ubiquity of chaos, ed. S. Krasner (American Association for the Advancement of Science, Washington, D.C., 1990), p. 23.
5 G. Matsumoto, K. Aihara, M. Ichikawa and A. Tasaki, J. Theor. Neurobiol. 3 (1984) 1.
6 K. Aihara, G. Matsumoto and Y. Ikegaya, J. Theor. Biol. 109 (1984) 249.
7 K. Aihara, G. Matsumoto and M. Ichikawa, Phys. Lett. A 111 (1985) 251.
8 K. Aihara, T. Numajiri, G. Matsumoto and M. Kotani, Phys. Lett. A 116 (1986) 313.
9 K. Aihara and G. Matsumoto, in: Chaos, ed. A.V. Holden (Manchester Univ. Press, Manchester, 1986) p. 257.
10 K. Aihara, M. Kotani and G. Matsumoto, in: Structure, coherence and chaos in dynamical systems, eds. P.L. Christiansen and R.D. Parmentier (Manchester Univ. Press, Manchester, 1989) p. 613.
11 M.R. Guevara, L. Glass and A. Shrier, Science 214 (1981) 1350.
12 A. Babloyantz, J.M. Salazar and C. Nicolis, Phys. Lett. A 111 (1985) 152.
13 H. Hayashi, M. Nakao and K. Hirakawa, Phys. Lett. A 88 (1982) 265.
14 H. Hayashi, S. Ishizuka, M. Ohta and K . Hirakawa, Phys. Lett. A 88 (1982) 435.
15 H. Hayashi, S. Ishizuka and K. Hirakawa, J. Phys. Soc. Jpn. 55 (1986) 3272.
16 D.R. Chialvo, R.F. Gilmour Jr and J. Jalife, Nature 343 (1990) 653.
17 T.R. Chay and J. Rinzel, Biophys. J. 47 (1985) 357.
18 T.R. Chay, Physica D 16 (1985) 233.
19 K. Aihara and G. Matsumoto, in: Chaos in biological systems, eds. H. Degan, A.V. Holden and L.F. Olsen (Plenum Press, New York, 1987) p. 121.
20 T.R. Chay and Y.S. Lee, Biophys. J. 47 (1985) 641.
21 A. Lahiri, D.K. Goswami, U. Basu and B. Dasgupta, Phys. Lett. A 111 (1985) 246.
22 R. Blumenthal, J. Theor. Biol. 49 (1975) 219.
23 T.R. Chay, J. Theor. Biol. 80 (1979) 83.
24 A. Karlin, J. Theor. Biol. 16 (1967) 306.
25 H. Kijima and S. Kijima, J. Theor. Biol. 71 (1978) 567.
26 T. Uemura and T. Ishii, Chem. Phys. Lett. 151 (1988) 217.
27 K. Hayashi, K. Toko and K. Yamafuji, Jpn. J. Appl. Phys. 28 (1989) 1507.
28 K. Toko, T. Matsuno, Y. Saida, K. Hayashi, S. Iiyama and K. Yamafuji, in: Noise in physical systems and $1/f$ fluctuations, eds. T. Musha, S. Sato and M. Yamamoto (Ohmsha, Tokyo, 1991) p. 629.
29 K. Toko, Y. Saida, T. Matsuno, K. Hayashi and K. Yamafuji, Proc. of 2nd Int. Conf. on Fuzzy Logic and Neural Networks (Iizuka, Japan, July 1992) p. 943.
30 T. Uemura and T. Ishii, J. Surface Sci. Technol. in press.
31 T. Kawakubo, Biophys. Chem. 23 (1986) 229.
32 R. De Levie, Adv. Chem. Phys. 37 (1978) 99.
33 G. Nicolis and I. Prigogine, Self-organization in nonequilibrium systems (Wiley, New York, 1977) Chap. 7.
34 P. Grassberger and I. Procaccia, Phys. Rev. Lett. 50 (1983 346.
35 B.C. So and H. Mori, Prog. Theor. Phys. 72 (1984) 1258.
36 J.S. Turner, J.C. Roux, W.D. McCormich and H.L. Swinney, Phys. Lett. A 85 (1981) 9.
37 N. Kamo, T. Yoshioka, M. Yoshida and T. Sugita, J. Membr. Biol. 12 (1973) 193.
38 M. Yoshida, N. Kamo and Y. Kobatake, J. Membr. Biol. 8 (1972) 389.
39 M. Miyake and K. Kurihara, Biochim. Biophys. Acta 762 (1983) 256.
40 S.H. Heinemann and F.J. Sigworth, Biophys. J. 57 (1990) 499.
41 A. Naparstek, D. Thomas and S.R. Caplan, Biochim. Biophys. Acta 323 (1973) 643.
42 S. Iiyama, K. Toko and K. Yamafuji, Biophys. Chem. 28 (1987) 129.
43 R. Rosen, Dynamical system theory in biology, Vol. 1 (Wiley, New York, 1970) Chap. 7.